Journal of Applied Pharmaceutical Research
Volume 13 Issue 2, Year of Publication 2025, Page 172 – 180
DOI: https://doi.org/10.69857/joapr.v13i2.1093

Check for updates

Research Article

JOURNAL OF APPLIED PHARMACEUTICAL RESEARCH | JOAPR
www.japtronline.com *ISSN: 2348 – 0335*

DEVELOPMENT AND CHARACTERISATION OF LYOPHILISED ETHAMBUTOL-LOADED POLYMERIC NANOPARTICLES

Eknath Kole[1], Yogesh Sonar[2], Rahul J. Sarode[3], Atul Chaudhari[1], Jitendra Naik[1]*

Article Information
Received: 13th January 2025
Revised: 29th March 2025
Accepted: 16th April 2025
Published: 30th April 2025

Keywords
Ethambutol, Poly-Ɛ-caprolactone, Lyophilization, Sustained release, Tuberculosis.

ABSTRACT
Background: Tuberculosis (TB) remains a universal health crisis, requiring innovative drug delivery systems to overcome challenges like prolonged treatment duration and patient non-adherence. This study was designed to develop Ethambutol (ETH)-loaded poly-ε-caprolactone (PCL) nanoparticles (NPs) as a sustained-release pulmonary delivery platform for TB therapy. **Methodology**: ETH-PCL NPs were fabricated using the nanoprecipitation technique with Lutrol® F68 as a stabiliser. The formulation was optimised for physicochemical properties (particle size, polydispersity index (PDI), zeta potential), encapsulation efficiency (EE), and morphology (SEM). *In vitro* drug release and 3-month colloidal stability were evaluated. **Results and Discussion**: The optimised NPs exhibited a rod-shaped morphology with smooth surfaces, an average size of 426.3 ± 13.03 nm, PDI < 0.467, zeta potential of -18.8 ± 0.520 mV, and EE of 76.57±3.86%. Sustained ETH release (86.62% over 24 h) and robust colloidal stability (negligible changes in size, PDI, and zeta potential over 3 months) were achieved. The formulation's biodegradable PCL core and scalable design align with the need for cost-effective, patient-centric therapies. **Conclusion**: ETH-PCL NPs represent a promising nanocarrier platform for TB, combining sustained drug release, high encapsulation efficiency, and long-term stability. While in vitro results are encouraging, future studies must validate in vivo efficacy and pulmonary delivery potential. This work underscores the viability of nanotechnology in addressing TB treatment challenges, particularly in improving adherence and targeting mycobacteria-laden macrophages.

INTRODUCTION

Tuberculosis (TB), an infection caused by the *Mycobacterium tuberculosis* (Mtb), remains a major global health challenge. Despite sustained efforts to curb the disease, TB continues to exert a devastating impact worldwide. According to the World Health Organization's 2024 report, a projected 10.8 million new TB cases and nearly 1.25 million deaths attributed to the disease were recorded in 2023, underscoring the urgent need for enhanced therapeutic strategies [1–3]. Effective tuberculosis management requires therapeutic strategies simultaneously

[1]*Department of Pharmaceutical Technology, University Institute of Chemical Technology, Kavayitri Bahinabai Chaudhari North Maharashtra University, Jalgaon MS 425001, India.*
[2]*Department of Pharmaceutics, R. C. Patel Institute of Pharmacy, Shirpur, MS 425405, India*
[3]*Department of Pharmaceutics, R. C. Patel Institute of Pharmaceutical Education and Research, Shirpur, MS 425405, India.*

For Correspondence:** **jbnaik@nmu.ac.in

targeting dormant bacterial reservoirs in granulomatous lesions and actively replicating pathogens in necrotic lesions, necessitating multimodal treatment approaches [4]. Standard antitubercular therapy adheres to a biphasic regimen, initiating with a 2-month intensive phase combining four core first-line antimicrobial agents (isoniazid, rifampicin, pyrazinamide, and Ethambutol), followed by a 4-month continuation phase utilising isoniazid and rifampicin [5]. The prolonged duration of therapy (4–6 months) and the high pill burden associated with standard regimens often lead to clinical complications. These encompass reduced treatment adherence due to drug-related toxicity and drug-drug interactions, factors that predispose to suboptimal therapeutic responses and the progression of antimicrobial resistance in Mycobacterium tuberculosis [6].

Adherence to tuberculosis therapy is hindered by multifaceted barriers such as the complexity of multidrug protocols, socioeconomic burdens, and systemic side effects. These challenges are amplified by the unpalatable formulations of many antitubercular medications, disproportionately affecting pediatric populations. Dose omissions due to poor tolerability risk therapeutic inefficacy, and may foster the evolution of drug-resistant pathogens [7,8]**.** To address persistent barriers in tuberculosis management, such as poor patient adherence, drug toxicity, and resistance, evolution-pharmaceutical engineering advancements have enabled the development of targeted drug delivery systems, such as polymeric nanoparticles, lipid-based vesicles, and microparticulate carriers. These platforms aim to enhance therapeutic efficacy by improving bioavailability, reducing dosing frequency, and mitigating adverse effects through controlled drug release [9–13]. Nanocarrier-based drug delivery systems provide improved drug-loading capacity, tunable release kinetics, and targeted tissue-specific delivery while retaining the high biocompatibility required for clinical translation [14,15]. Polymeric nanocarriers have opened new avenues in precision medicine by leveraging their biodegradable nature and compatibility with the body's transport pathways. These systems can exploit features like increased vascular permeability in affected tissues to improve drug accumulation at the target site. At the same time, their extended circulation time helps maintain consistent therapeutic drug levels in the bloodstream [16,17]. Poly-ε-caprolactone (PCL) is widely recognised among synthetic biodegradable polymers for its suitability in drug delivery applications, thanks to a distinct set of pharmaceutical benefits. Its established biocompatibility, controllable degradation rate, and versatility in formulation design make it highly favourable for nanoparticle fabrication. The polymer's hydrophobicity and permeability are advantageous for prolonged drug release [18,19]. The use of combination polymers like PCL and Lutrol® F68 optimises drug delivery: PCLs biodegradable context ensures controlled/ sustained release of therapeutics, while Lutrol® F68 enhances nanoparticles stability by reducing opsonisation and improving hydrophilicity, collectively enabling precise macrophages-targeted intracellular delivery with reduced systemic dosing [20,22].

We developed Ethambutol (ETH)-loaded poly-ε-caprolactone (PCL) nanoparticles (ETH-PCL NPs) using the nanoprecipitation technique, followed by lyophilisation to enhance stability. Detailed physicochemical characterisation confirmed the formulation's optimal properties, including uniform particle size, acceptable colloidal stability, and high drug encapsulation efficiency. The optimised nanoparticles exhibited a sustained release profile of ETH, effectively addressing critical challenges in tuberculosis therapy, such as the need for prolonged drug exposure, reduced dosing frequency, and improved patient adherence. These results highlight the likelihood of the ETH-PCL nanocarrier system being a promising approach for advancing TB therapy.

MATERIALS AND METHODS

***Materials*:** Ethambutol (ETH) was gifted by Lupin Ltd. (Chhatrapati Sambhajinagar, India). Poly(ε-caprolactone) (PCL) and Lutrol® F68 were sourced from Sigma-Aldrich (USA) and BSAF, Ludwigshafen, Germany, respectively. Key solvents such as methanol, acetone, and glacial acetic acid, as well as sodium chloride, potassium chloride, hydrochloric acid, and sodium hydroxide, were acquired from Sisco Research Laboratories Pvt. Ltd. (Mumbai, India). Buffer components, including disodium hydrogen phosphate and potassium dihydrogen phosphate, were procured from Merck India. All chemicals were of analytical-grade quality.

***Preparation of Nanoparticles*:** The ETH-PCL NPs were synthesised using the nanoprecipitation technique. Initially, 100 mg of PCL was dissolved in acetone under bath sonication for 15 minutes to form the organic phase. Concurrently, an aqueous phase was prepared by dissolving 0.1% (w/w) Lutrol® F68 in double-distilled water. Separately, 50 mg of ETH was thawed in

5 mL of double-distilled water and added dropwise to the aqueous phase under stirring. Both phases were stirred individually at 600 rpm for 30 min and filtered through a 0.45 µm membrane filter. The nanoprecipitation process was carried out by slowly adding the organic phase into the aqueous phase under continuous magnetic stirring (400 rpm) at room temperature. Upon mixing, the spontaneous formation of nanoparticles occurred due to solvent diffusion and polymer precipitation [21,23].

The resulting ETH-PCL NPs were separated via three washes (centrifugation cycles) at 10,000 × g for 60 min at 4°C, with resuspension in fresh [solvent] after each cycle to ensure thorough purification. Blank PCL nanoparticles were prepared in parallel using the same method, excluding the drug. Following centrifugation, the nanoparticle suspension was pre-frozen at -20°C for 12 hours and then lyophilised at -60°C under 0.9 KPa vacuum pressure for 48 hours using a vacuum freeze-dryer (Boyikang Laboratory Instruments Inc., China). The final product was obtained as a dry, free-flowing powder and kept in amber glass vials in a desiccator at 25 ± 2°C till further characterisation.

***Particle Size, Polydispersity Index and Surface charge*:** Physicochemical characterisation of ETH-PCL NPs was performed using dynamic light scattering (DLS) (Nano ZS 90 Zetasizer, Malvern Instruments, UK) to assess hydrodynamic diameter, polydispersity index (PDI), and zeta potential. Samples were appropriately diluted with deionised water (approximately 1:10 ratio; at 7.0 pH) and measured at 25 °C using a 173° backscatter angle [24]; data were reported as mean ± standard deviation (SD) from triplicate (n=3).

Encapsulation Efficiency (EE) and Drug Loading (DL): The EE% and DL% of ETH-PCL NPs were measured using UV-visible spectrophotometry (UV-2600i, Shimadzu, Japan). The unentrapped drug was separated by centrifuging the nanoparticle suspension at 10,000 × g for 60 min at 4°C (Sorvall ST 8R, Thermo Scientific). The resulting supernatant was analysed at 272 nm using UV-Vis spectroscopy, with pure ETH quantified via a validated calibration curve (R^2 = 0.998) [21]. EE% and DL% were calculated using established equations, with all measurements conducted thrice (n = 3) and stated as mean ± SD.

$$\boldsymbol{Drug\ Loading}\left(\%\frac{\boldsymbol{w}}{\boldsymbol{w}}\right) = \frac{\boldsymbol{Weight\ of\ entraped\ ETH}}{\boldsymbol{Weight\ of\ nanoparticles}}\boldsymbol{X100}$$

$$\boldsymbol{Entrapment\ Efficiency}\ (\%) = \frac{\boldsymbol{Total\ ETH\ added - unbound\ ETH}}{\boldsymbol{Total\ ETH\ added}}\boldsymbol{X100}$$

***Particle morphology*:** Morphological evaluation of ETH-PCL NPs was conducted using field emission scanning electron microscopy (FE-SEM; JSM-IT300LV, JEOL, Japan). Before imaging, samples were sputter-coated with a 10 nm layer of gold via a JCE-3000FC coating unit (JEOL, Japan) for 50 seconds to enhance conductivity. Imaging was done at an accelerating voltage of 10 kV in secondary electron detection mode [25].

Redispersibility: The redispersibility of lyophilised ETH-PCL-NPs into nanoparticles was evaluated using a previously established method [21]. Briefly, the freeze-dried powder (2 mg) was reconstituted in 2 mL of ultrapure water under magnetic stirring (30 minutes), and the resulting nanosuspension was analysed for particle size using DLS. The redispersibility index (RDI), a metric quantifying the ability of the formulation to regain its original nanoparticle dimensions post-lyophilisation, was calculated as follows:

$$\boldsymbol{Redispersibility\ index}\ (\boldsymbol{RDI}) = \frac{\boldsymbol{Average\ particle\ szie\ of\ nanosupension}}{\boldsymbol{Average\ particle\ size\ of\ freeze\ dried\ powder}}$$

Fourier transform infrared Spectroscopy (FT-IR): FT-IR study was conducted with a PerkinElmer Spectrum Two Spectrometer (USA) coupled with a universal attenuated total reflectance (ATR) attachment (diamond/ZnSe crystals). Samples analysis was performed in transmission mode at a resolution of 4 cm^{-1}, with 16 accumulated scans per measurement under a constant dry air purge to minimise moisture interference [26]. The mid-infrared spectral range (400-400 cm^{-1}) was examined for pure ETH, PCL, Lutrol® F68, and ETH-PCL-NPs formulation to assess functional group interactions.

X-ray diffraction study (XRD): The crystallinity and physical state of the samples were evaluated via an X-ray diffractometer (D8 Focus, Bruker AXS) coupled with a Cu Kα radiation source (λ = 1.5406 Å). The instrument operated at 40 kV and 40 mA. Powdered samples of pure ETH, PCL, Lutrol® F68, and the ETH-PCL NPs formulation were uniformly distributed in plastic sample holders and gently levelled using a glass slide [27,28]. XRD measurements were conducted at room temperature over a 2θ range of 5° to 60° and a scanning speed of 1°/min.

***In vitro drug release and kinetic study*:** *In vitro* drug release studies of pure ETH and ETH-PCL NPs were conducted under sink conditions by the dialysis bag diffusion method (MWCO 12–14 kDa; Sigma-Aldrich). A 2 mL sample containing the equivalent of 50 mg ETH was placed into pre-soaked dialysis bags and deep in 900 mL of phosphate-buffered saline (PBS, pH 7.4) kept at 37.5 ± 0.5 °C with constant agitation at 50 rpm. 5 mL of the release medium was withdrawn and instantly exchanged at fixed time points with a corresponding volume of fresh PBS to uphold sink conditions [29,30]. Samples were passed through 0.2 µm PVDF syringe filters to eliminate any residual particulates, and the content of ETH was calculated by UV-visible spectrophotometry at 272 nm. The result was presented in triplicate (n = 3) as mean ± SD.

***Stability study*:** The stability of ETH-PCL NPs was assessed over 3 months under storage conditions at 25°C. Formulations stored in sealed amber vials were evaluated monthly for variations in particle size, PDI, and zeta potential to monitor their physicochemical stability [31].

***Statistical analysis*:** The experimental data are presented as the mean ± SD from triplicate independent measurements.

RESULTS AND DISCUSSION

Particle Size, Polydispersity Index and Surface Charge: The optimised ETH-PCL NPs formulation demonstrated favourable physicochemical characteristics, with an average particle size of 423.6 ± 130.3 nm (Figure 1A**)**, confirming successful nanoparticle formation. The PDI of 0.467 ± 0.131 indicated a homogeneous size distribution, while the zeta potential of -18.8 ± 0.520 mV (Figure 1B) suggested good colloidal stability. These findings confirm the efficacy of the nanoprecipitation method in producing ETH-PCL NPs with desirable properties. Particle size (220.3 ± 2.6 nm), PDI (0.25 ± 0.1), and zeta potential (-19.5 ±0.9) align with previously reported values for PCL nanoparticles stabilised with non-ionic surfactants such as Lutrol® F68 [32]. These parameters reflect the characteristics, stability, and polydispersity of PCL-based systems, ensuring suitability for targeted therapeutic delivery.

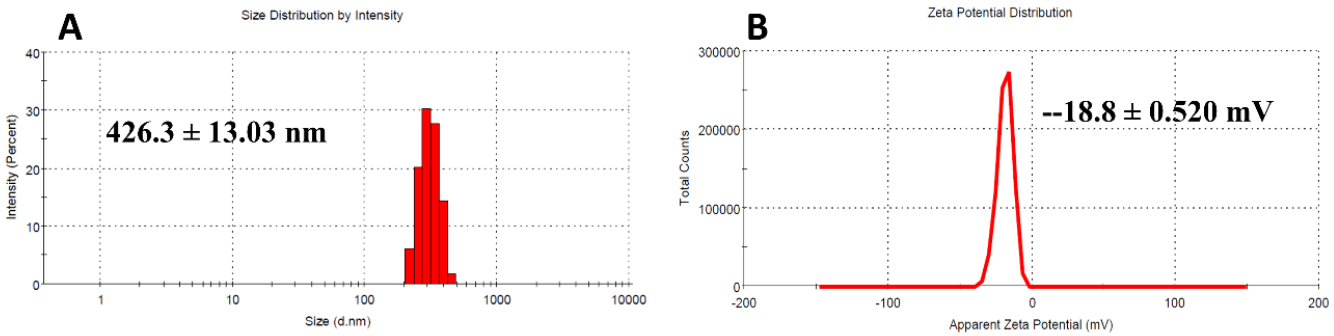

Figure 1. Physicochemical characterisation of ETH-PCL NPs: A) Average particle size, B) zeta potential, by dynamic light scattering, DLS, Data represented mean ± SD (n = 3).

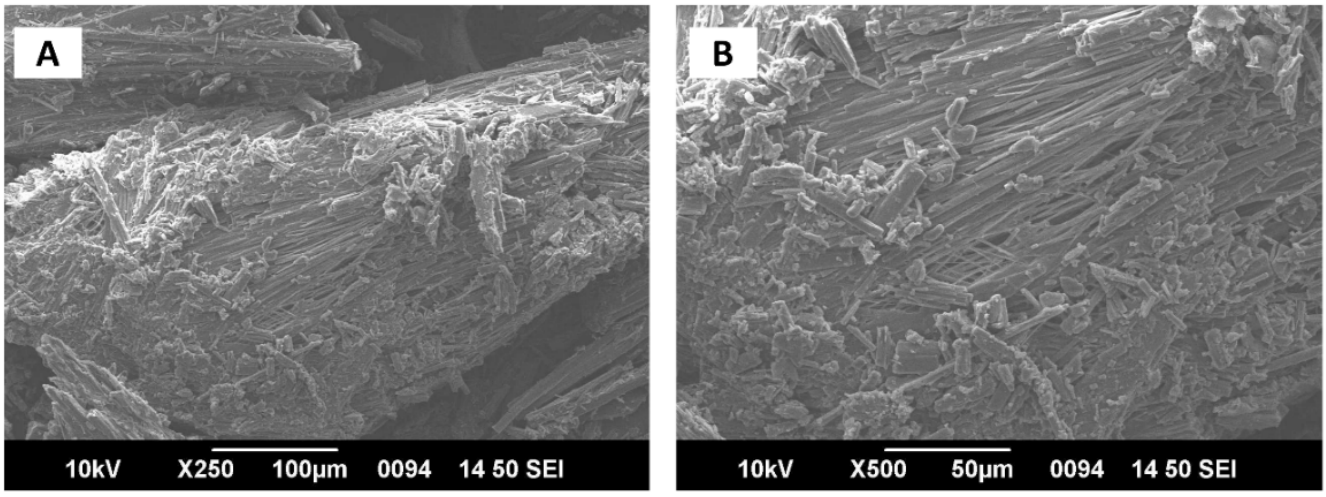

Figure 2: (A) SEM images of ETH-PCL-NPS showing rod-like structure (B) Scale bar: 100 and 50 µm; acceleration voltage: 10 kV

Entrapment Efficiency (EE) and Drug Loading (DL): The EE% of the lyophilised ETH-PCL NPs was determined by analysing the supernatant to quantify the unencapsulated ETH in the aqueous phase and comparing it with the initial drug loading. The formulation exhibited a high drug encapsulation efficiency of 76.57 ± 3.86% and a drug loading capacity of 12.43 ± 0.39% w/w (mean ± SD, n = 3). These results demonstrate the entrapment of ETH into the polymeric matrix, emphasising the formulation's effective drug-loading potential.

***Particle Morphology*:** The SEM images of the lyophilised ETH-PCL NPs formulation revealed a rod-shaped morphology with a smooth surface. Smaller particles were observed to adhere to the larger ones, indicating some degree of agglomeration (Figure 2 A and B)

Redispersibility: A redispersibility study was performed to assess the ability of lyophilised ETH-PCL-NPs powder to reform nanoparticles in aqueous solution. Reconstitution of the freeze-dried formulation yielded nanoparticles with an average particle size of 421.4 ± 0.8 nm, PDI of 0.358 ± 0.041, and surface charge of -20.7 ± 2.16 mV, confirming colloidal stability. The RDI, a critical metric for evaluating reconstitution efficiency, was calculated as 1.026 for the formulation. This value, approximating unity, signifies minimal particle aggregation and excellent redispersion potential. Comparative analysis of pre- and post-lyophilisation particle sizes via RDI confirmed no significant changes, demonstrating the robustness of the freeze-drying process.

Fourier transform infrared Spectroscopy (FT-IR): FTIR spectrum of ETH shows distinctive peaks conforming to its functional groups: O-H stretching vibrations at 3289.20 cm^{-1}, N-H stretching at 3305.50 cm^{-1}, -C≡N stretching at 2253.21 cm^{-1}, C=O stretching at 1656.20 cm^{-1}, N-H bending at 1630.20 cm^{-1}, pyridine ring vibrations at 1405.20 cm^{-1}, free NH2 stretching at 1214.16 cm^{-1}, and -CH_3 stretching at 1136.47 cm^{-1}, confirming its molecular structure. For PCL, characteristics peaks include asymmetric CH_2 stretching at 2933.46 cm^{-1}, symmetric CH_2 stretching at 2852.46 cm^{-1}, C=O stretching at 1817.51 cm^{-1}, and asymmetric COC/C-C/C-O stretching vibrations at 1719.40 cm^{-1}, 1614.46 cm^{-1}, and 1169.81 cm^{-1} respectively. Lutrol® F68 exhibits peaks for O-H stretching at 2986.43 cm^{-1}, aliphatic C-H stretching at 2881.27 cm^{-1}, in-plane O-H bending at 1359.34 cm^{-1}, and C-O stretching at 2180.72 cm^{-1}, consistent with its structure. The ETH-PCL-NPs spectrum reveals characteristics of absorption bands: the broad peak at 3307.32 cm^{-1} corresponds to overlapping O-H/N-H stretching vibrations from ETH and Mannitol, while the shifted C=O stretch at 1738.78 cm-1 (from PCL) and N-H bending at 1558.79 cm^{-1} (from ETH) suggest non-covalent interactions via hydrogen bonds. Pelas at 2937.23/2881.87 cm^{-1} (CH_2 stretches) and 1108-1077 cm^{-1} (C-O vibrations) reflect preserved molecular characteristics of PCL and Mannitol, with no new chemical bonds detected, confirming the physical stabilisation of the nanoparticle matrix (Figure 3).

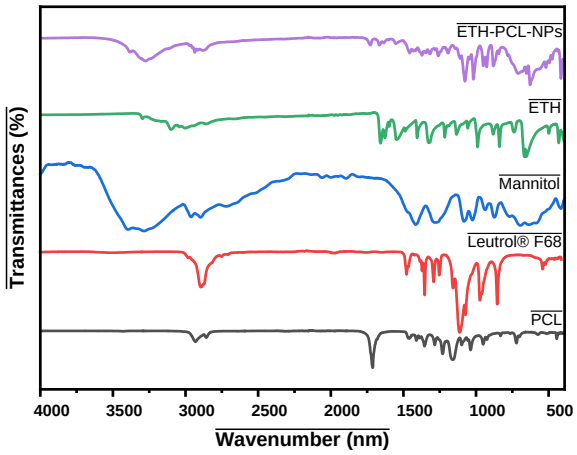

Figure 3: FTIR spectrum of pure drug, excipient and ETH-PCL-NPs

***X-ray diffraction analysis*:** Figure 4 revealed distinct crystallinity in pure ETH, with sharp peaks at 8.08°, 15.71°, 20.88°, 22.39°, 23.42°, 27.18°, 31.73°, and 41.72°, confirming its highly crystalline nature. PCL and Lutrol® F68 exhibited characteristic peaks at 22.33°, 24.65°, and 19.51°, 23.68°, respectively.

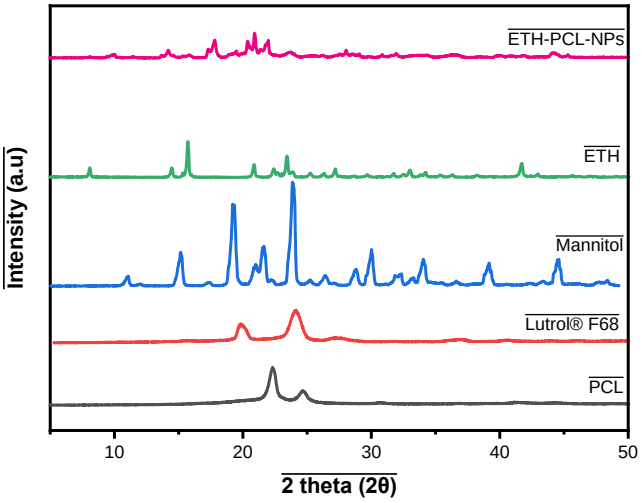

Figure 4 X-ray diffraction (XRD) patterns

In contrast, the ETH-PCL NPs showed a modified diffraction pattern with broader, less intense peaks at 14.24°, 17.86°, 20.96°, 22.03°, and 28.09°, indicating a significant reduction in ETH crystallinity and partial amorphization occur upon the drug's encapsulation in a polymeric matrix. The absence of sharp ETH peaks and the slight broadening of PCL reflections suggest successful drug incorporation and molecular dispersion within the polymer matrix.

***In-vitro drug release study*:** The *in vitro* release study executed in PBS (pH 7.4) by the dialysis bag method demonstrated distinct release behaviours for pure ETH and the ETH-PCL NPs. Pure ETH showed a rapid and immediate release, with approximately 94.46% of the drug released within the initial 2 hours. Conversely, the ETH-PCL NPs exhibited a sustained release pattern, with only 22.16% released at 2 hours and a cumulative release of 86.62% over 24 hours (Figure 5 A**).** This sustained release profile underscores the capability of the PCL matrix to prolong drug release, potentially maintaining therapeutic levels for extended periods.

Such a controlled delivery approach presents clear advantages in tuberculosis therapy by reducing the frequency of administration and enhancing patient adherence.

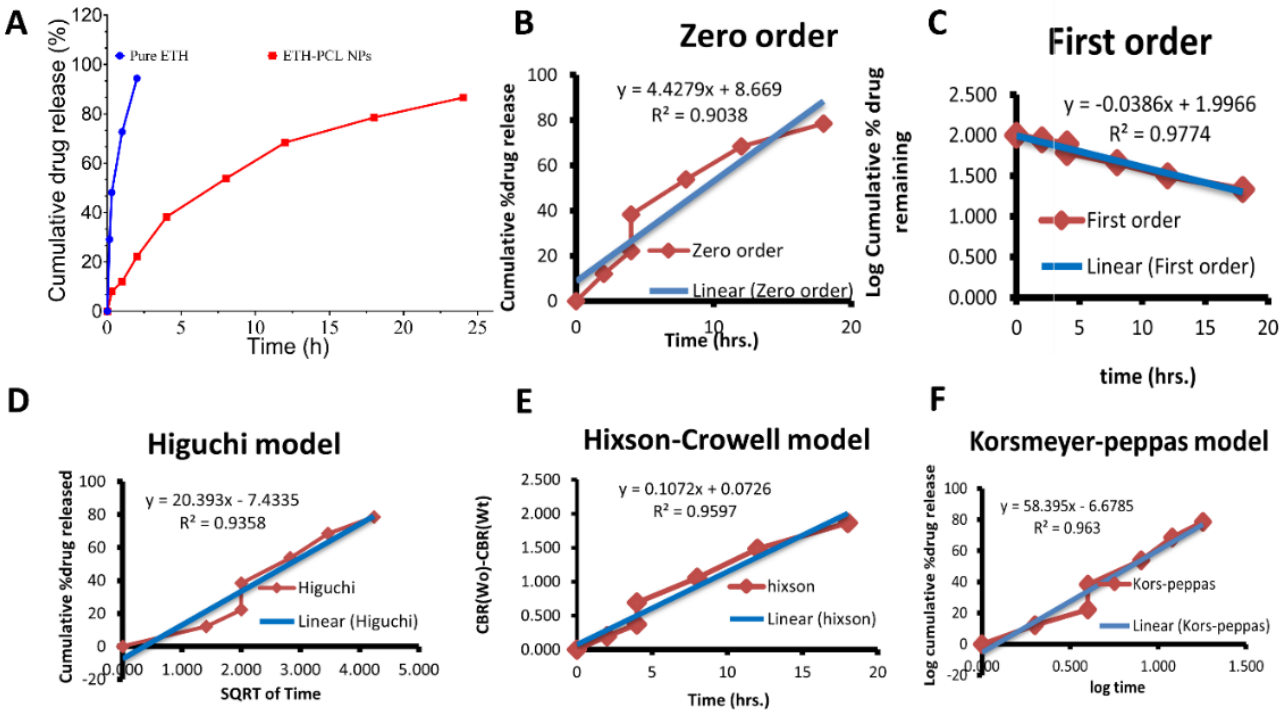

Figure 5 A) *In vitro* release of pure ETH and ETH-PCL NPs (n = 3; mean ± SD). In vitro release kinetic study, B) Zero order kinetic model, C) First order kinetic model, D) Korsmeyer-Peppas model, E) Hixson-Crowell model, and F) Higuchi model

In vitro release kinetic study: The drug release kinetics exhibited a hybrid mechanism, predominantly governed by first-order kinetics (R^2 = 0.9774), signifying concentration-dependent release with an initial burst phase. The robust fit to the Korsmeyer-Peppas model (R^2 = 0.963) denotes anomalous transport (non-Fickian diffusion) involving concurrent diffusion and polymer relaxation/erosion mechanisms. Simultaneously, the Hixson-Crowell model correlation (R^2 = 0.9597) highlights a partial surface erosion mechanism, while adherence to the Higuchi model (R^2 = 0.9358) reinforces diffusion-controlled release within a matrix-based system. The comparatively low zero-order fit (R^2 = 0.9038) underscores deviations from constant release kinetics (Figure 5 B-F). The data suggest a biphasic release pattern: an initial rapid dissolution phase, succeeded by a sustained release phase mediated by diffusion and erosion mechanisms.

***Stability study*:** The stability of lyophilised ETH-PCL NPs was assessed over 3 months under ambient storage conditions (25 ± 2 °C). During this period, essential properties like particle size, zeta potential, and PDI stayed stable with no significant changes. These results confirm the long-term stability of the

nanoparticle system, supporting its suitability for extended storage without compromising formulation quality (Figure 6A and B). In the study by Diwan et al., optimised Cilnidipine-loaded PCL-NPs retained consistent particle size, PDI, and zeta potential over three months, indicating robust colloidal stability [32]. Such outcomes align with prior findings for PLC systems stabilised with non-ionic surfactant, i.e., Lutrol® F68, where negligible size fluctuation and stable surface charge ensure long-term storage stability.

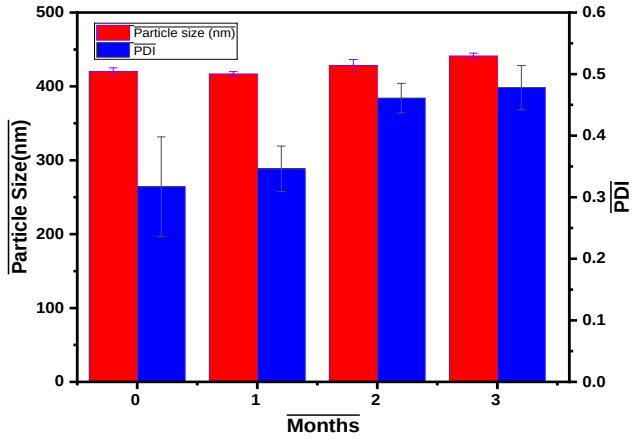

Figure 6: A) Stability study of ETH-PCL NPs (Particle size and PDI) (mean ± SD, n=3)

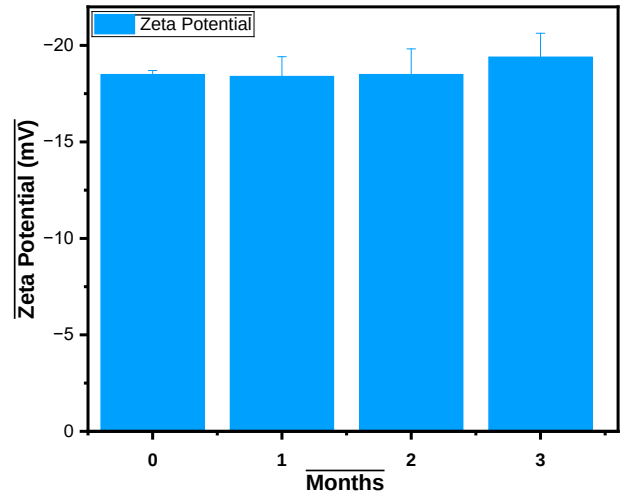

Figure 6: B) Stability study of ETH-PCL NPs (surface charge) (mean ± SD, n=3).

CONCLUSIONS

In this study, ethambutol (ETH)-loaded poly-ε-caprolactone (PCL) nanoparticles (NPs) were successfully developed using the nanoprecipitation technique, with Lutrol® F68 as a stabiliser to address the challenges of conventional Tuberculosis (TB) therapy. The optimised nanoformulation exhibited favourable physicochemical properties, including a uniform rod-shaped morphology (426.3 ± 13.03 nm), low polydispersity (PDI < 0.467), moderate zeta potential (-18.8 ± 0.520 mV), and high encapsulation efficiency (76.57 ± 3.86%). *In vitro* release studies demonstrated sustained ETH release (86.62% over 24 h), while stability assessments confirmed minimal changes in particle size, PDI, and zeta potential over three months, underscoring robust colloidal stability. Our developed nanoformulation addresses critical TB therapy challenges by sustained drug release, reducing dose frequency and using biodegradable PLC nanoparticles to improve the adherence and macrophage-targeted delivery. Moreover, limited to in vitro data, future studies will evaluate the *in vivo* efficacy of the nanoparticles in a murine model of tuberculosis.

ACKNOWLEDGEMENTS

The authors thank BARTI, Pune, for providing the Dr. Babasaheb Ambedkar National Research Fellowship (BANRF) and gratefully acknowledge Lupin Ltd. (Cha. Sambhajinagar, India) for providing the gift sample of Ethambutol.

FINANCIAL ASSISTANCE

The Science and Engineering Research Board (SERB), New Delhi, financially supported this study through Empowerment and Equity Opportunities for Excellence in Science (EEQ/2023/000060).

CONFLICT OF INTEREST

The authors declare no conflict of interest.

AUTHOR CONTRIBUTION

Eknath Kole contributed to conceptualization, experimentation, data curation, and original draft writing. Yogesh Sonar and Rahul Sarode contributed to the experimentation. Atul Chaudhari contributed to experimentation and image preparation. Jitendra Naik wrote, reviewed, and edited the manuscript. He also contributed to project administration, funding acquisition, and supervision.

REFERENCES

[1] Bahlool AZ, Cavanagh B, Sullivan AO, MacLoughlin R, Keane J, Sullivan MPO, Cryan SA. Microfluidics produced ATRA-loaded PLGA NPs reduced tuberculosis burden in alveolar epithelial cells and enabled high delivered dose under simulated human breathing pattern in 3D printed head models. *Eur. J.*

Pharm. Sci., **196**, 106734 (2024) https://doi.org/10.1016/j.ejps.2024.106734.

[2] Sefat KMSR, Kumar M, Kehl S, Kulkarni R, Leekha A, Paniagua MM, Ackart DF, Jones N, Spencer C, Podell BK, Ouellet H, Varadarajan N. An intranasal nanoparticle vaccine elicits protective immunity against Mycobacterium tuberculosis. *Vaccine*, **42**, (2024) https://doi.org/10.1016/j.vaccine.2024.04.055.

[3] Estaji F, Kamali A, Keikha M. Strengthening the global Response to Tuberculosis: Insights from the 2024 WHO global TB report. *J Clin Tuberc Other Mycobact Dis*, **39**, 100522 (2025) https://doi.org/10.1016/j.jctube.2025.100522

[4] Chee CBE, Reves R, Zhang Y, Belknap R. Latent tuberculosis infection: Opportunities and challenges. *Respirology*, **23**, 893–900 (2018) https://doi.org/10.1111/resp.13346.

[5] Mobed A, Alivirdiloo V, Gholami S, Moshari A, Mousavizade A, Naderian R, Ghazi F. Nano-Medicine for Treatment of Tuberculosis, Promising Approaches Against Antimicrobial Resistance. *Curr. Microbiol.*, **81**, 1–15 (2024) https://doi.org/10.1007/s00284-024-03853-z.

[6] Patil SM, Diorio AM, Kommarajula P, Kunda NK. A quality-by-design strategic approach for the development of bedaquiline-pretomanid nanoparticles as inhalable dry powders for TB treatment. *Int. J. Pharm.*, **653**, 123920 (2024) https://doi.org/10.1016/j.ijpharm.2024.123920.

[7] Fekadu G, Bekele F, Bekele K, Girma T, Mosisa G, Gebre M, Alemu T, Tekle T, Gamachu B, Diriba A. Adherence to Anti-Tuberculosis Treatment Among Pediatric Patients at Nekemte Specialized Hospital, Western Ethiopia. *Patient Prefer. Adherence*, **Volume 14**, 1259–65 (2020) https://doi.org/10.2147/PPA.S258292.

[8] Bea S, Lee H, Kim JH, Jang SH, Son H, Kwon J-W, Shin J-Y. Adherence and Associated Factors of Treatment Regimen in Drug-Susceptible Tuberculosis Patients. *Front. Pharmacol.*, **12**, (2021) https://doi.org/10.3389/fphar.2021.625078.

[9] Jadhav K, Kole E, Abhang A, Rojekar S, Sugandhi V, Verma RK, Mujumdar A, Naik J. Revealing the potential of nano spray drying for effective delivery of pharmaceuticals and biologicals. *Dry. Technol.*, 1–24 (2024) https://doi.org/10.1080/07373937.2024.2437691.

[10] Pardeshi SR, Kole EB, Kapare HS, Chandankar SM, Shinde PJ, Boisa GS, Salgaonkar SS, Giram PS, More MP, Kolimi P, Nyavanandi D, Dyawanapelly S, Junnuthula V. Progress on Thin Film Freezing Technology for Dry Powder Inhalation Formulations. *Pharmaceutics*, **14**, 2632 (2022) https://doi.org/10.3390/pharmaceutics14122632.

[11] Kole E, Jadhav K, Shirsath N, Dudhe P, Verma RK, Chatterjee A, Naik J. Nanotherapeutics for pulmonary drug delivery: An emerging approach to overcome respiratory diseases. *J. Drug Deliv. Sci. Technol.*, **81**, 104261 (2023) https://doi.org/10.1016/j.jddst.2023.104261.

[12] Jadhav K, Kole E, Singh R, Rout SK, Verma RK, Chatterjee A, Mujumdar A, Naik J. A critical review on developments in drying technologies for enhanced stability and bioavailability of pharmaceuticals. *Dry. Technol.*, **42**, 1415–41 (2024) https://doi.org/10.1080/07373937.2024.2357181.

[13] Kole E, Jadhav K, Sonar Y, Kapse M, Patil SA, Kumar A. Advances in spray drying technology for anti-tubercular formulation development : A comprehensive review. *Dry. Technol.*, **0**, 1–37 (2025) https://doi.org/10.1080/07373937.2024.2437690.

[14] Patra JK, Das G, Fraceto LF, Campos EVR, Rodriguez-Torres M del P, Acosta-Torres LS, Diaz-Torres LA, Grillo R, Swamy MK, Sharma S, Habtemariam S, Shin H-S. Nano based drug delivery systems: recent developments and future prospects. *J. Nanobiotechnology*, **16**, 71 (2018) https://doi.org/10.1186/s12951-018-0392-8.

[15] Kumar M, Virmani T, Kumar G, Deshmukh R, Sharma A, Duarte S, Brandão P, Fonte P. Nanocarriers in Tuberculosis Treatment: Challenges and Delivery Strategies. *Pharmaceuticals*, **16**, 1360 (2023) https://doi.org/10.3390/ph16101360.

[16] Begines B, Ortiz T, Pérez-Aranda M, Martínez G, Merinero M, Argüelles-Arias F, Alcudia A. Polymeric Nanoparticles for Drug Delivery: Recent Developments and Future Prospects. *Nanomaterials*, **10**, 1403 (2020) https://doi.org/10.3390/nano10071403.

[17] Eltaib L. Polymeric Nanoparticles in Targeted Drug Delivery: Unveiling the Impact of Polymer Characterization and Fabrication. *Polymers (Basel).*, **17**, 833 (2025) https://doi.org/10.3390/polym17070833.

[18] Opriș O, Mormile C, Lung I, Stegarescu A, Soran M-L, Soran A. An Overview of Biopolymers for Drug Delivery Applications. *Appl. Sci.*, **14**, 1383 (2024) https://doi.org/10.3390/app14041383.

[19] Tsung T-H, Tsai Y-C, Lee H-P, Chen Y-H, Lu D-W. Biodegradable Polymer-Based Drug-Delivery Systems for Ocular Diseases. *Int. J. Mol. Sci.*, **24**, 12976 (2023) https://doi.org/10.3390/ijms241612976.

[20] Alimohammadi M, Fakhraei O, Moradi A, Kabiri M, Moradi A, Passandideh-Fard M, Tamayol A, Ebrahimzadeh MH, Mousavi Shaegh SA. Controlled release of azithromycin from polycaprolactone/chitosan nanofibrous membranes. *J. Drug Deliv. Sci. Technol.*, **71**, 103246 (2022) https://doi.org/10.1016/j.jddst.2022.103246.

[21] Kole E, Jadhav K, Khan Z, Verma RK, Chatterjee A, Mujumdar A, Naik J. Engineered vildagliptin-loaded polymeric nanoparticles via microfluidic and spray drying for enhanced antidiabetic activity. *Futur. J. Pharm. Sci.*, **10**, 156 (2024) https://doi.org/10.1186/s43094-024-00736-9.

[22] Sun H, Mei L, Song C, Cui X, Wang P. The in vivo degradation, absorption and excretion of PCL-based implant. *Biomaterials*, **27**, 1735–40 (2006) https://doi.org/10.1016/j.biomaterials.2005.09.019.

[23] Patil A, Pardeshi S, Kapase M, Patil P, More M, Dhole S, Kole E, Deshmukh P, Gholap A, Mujumdar A, Naik J. Continuous preparation of sustained release vildagliptin nanoparticles using tubular microreactor approach. *Dry. Technol.*, 1–13 (2024) https://doi.org/10.1080/07373937.2023.2298778.

[24] Guo P, Buttaro BA, Xue HY, Tran NT, Wong HL. Lipid-polymer hybrid nanoparticles carrying linezolid improve treatment of methicillin-resistant Staphylococcus aureus (MRSA) harbored inside bone cells and biofilms. *Eur. J. Pharm. Biopharm.*, **151**, 189–98 (2020) https://doi.org/10.1016/j.ejpb.2020.04.010.

[25] Mandpe S, Kole E, Parate V, Chatterjee A, Mujumdar A, Naik J. Development, QbD-based optimisation, in-vivo pharmacokinetics, and ex-vivo evaluation of Eudragit ® RS 100 loaded flurbiprofen nanoparticles for oral drug delivery. *J. Microencapsul.*, 1–13 (2024) https://doi.org/10.1080/02652048.2024.2427294.

[26] Khairnar G, Mokale V, Khairnar R, Mujumdar A, Naik J. Production of antihyerglycemic and antihypertensive drug loaded sustained release nanoparticles using spray drying technique: Optimization by Placket Burman Design. *Dry. Technol.*, **40**, 626–37 (2022) https://doi.org/10.1080/07373937.2020.1825292.

[27] Mandpe S, Kole E, Parate V, Chatterjee A, Mujumdar A, Naik J. Design, development, and evaluation of spray dried flurbiprofen loaded sustained release polymeric nanoparticles using QBD approach to manage inflammation. *Dry. Technol.*, 1–13 (2023) https://doi.org/10.1080/07373937.2023.2251572.

[28] Mandpe S, Kole E, Parate V, Chatterjee A, Mujumdar A, Naik J. Development, QbD-based optimisation, in-vivo pharmacokinetics, and ex-vivo evaluation of Eudragit ® RS 100 loaded flurbiprofen nanoparticles for oral drug delivery. *J. Microencapsul.*, **0**, 1–13 (2024) https://doi.org/10.1080/02652048.2024.2427294.

[29] Jiang Y, Zhou Y, Zhang CY, Fang T. Co-delivery of paclitaxel and doxorubicin by ph-responsive prodrug micelles for cancer therapy. *Int. J. Nanomedicine*, **15**, 3319–31 (2020) https://doi.org/10.2147/IJN.S249144.

[30] Verma U, Mujumdar A, Naik J. Preparation of Efavirenz resinate by spray drying using response surface methodology and its physicochemical characterization for taste masking. *Dry. Technol.*, **38**, 793–805 (2020) https://doi.org/10.1080/07373937.2019.1590845.

[31] Wagh P, Mujumdar A, Naik JB. Preparation and characterization of ketorolac tromethamine-loaded ethyl cellulose micro-/nanospheres using different techniques. *Part. Sci. Technol.*, **37**, 347–57 (2019) https://doi.org/10.1080/02726351.2017.1383330.

[32] Diwan R, Ravi PR, Agarwal SI, Aggarwal V. Cilnidipine loaded poly (ε-caprolactone) nanoparticles for enhanced oral delivery: optimization using DoE, physical characterization, pharmacokinetic, and pharmacodynamic evaluation. *Pharm. Dev. Technol.*, **26**, 278–90 (2021) https://doi.org/10.1080/10837450.2020.1864643.